CONFERENCE PRE-PRINT

NUMERICAL ANALYSIS OF ELECTRON DISTRIBUTION FUNCTION UNDER ELECTRON CYCLOTRON HEATING DURING TOKAMAK START-UP

N. TSUJII, A. EJIRI, K. SHINOHARA, Y. PENG, Y. LIN, Z. JIANG, Y. TIAN, F. ADACHI, Y. JIANG, S. WANG, M. YOSHIDA and Y. TAKECHI

The University of Tokyo Kashiwa, Japan

Email: tsujii@k.u-tokyo.ac.jp

Abstract

Electron cyclotron (EC) heating has been considered necessary for the start-up of a large tokamak with a superconducting central solenoid (CS) due to its limited loop voltage. Recently, the trapped-particle configuration (TPC) that confines collisionless electrons was found to be effective for EC assisted start-up. The global phase-space structure of collisionless electrons during TPC start-up was analyzed in terms of the orbit-averaged distribution function. Transport of collisionless electrons generated by EC waves was simulated with orbit-averaged Fokker-Planck equation solver that can treat open field-lines. The result of the Fokker-Planck simulation was introduced to equilibrium reconstruction code based on extended magnetohydrodynamics (MHD) that included the kinetic electron current. Finite orbit effects and relativistic effects were considered consistently for both the Fokker-Planck simulation and the extended MHD equilibrium reconstruction. Time evolution of the global electron distribution function was simulated for the first time starting from the vacuum TPC up to closed flux surface formation. The kinetic electron current generated by EC heating under the TPC was shown to be sufficient to form closed flux surfaces. The electron distribution function was predicted to have a characteristic phase-space structure resulting from strong acceleration of trapped electrons with turning points at the EC resonance layer. EC heating power was predicted to dominate over Ohmic heating power during this early start-up phase.

1. INTRODUCTION

Start-up of a large tokamak with a superconducting central solenoid (CS) is challenging due to its limited loop voltage. Electron Cyclotron (EC) heating has been considered necessary to assist Ohmic start-up at low loop voltage to initiate breakdown as well as to assist burn-through. In the early studies, EC heating was applied to the conventional field-null configuration (FNC) that was optimized for Ohmic breakdown [1]. More recently, the trapped particle configuration (TPC) that has been studied for fully non-inductive rf start-up [2,3] was found to be effective for EC assisted Ohmic start-up as well [4-7]. It was shown experimentally that the operational parameter space was expanded and that the plasma current rise was faster under the TPC compared to the conventional FNC. Improvement was particularly substantial at low neutral pressure and high EC power whereas the difference of the performance between the two configurations was insignificant at high neutral pressure [7]. These results suggested that collisionless trapped electrons generated by EC heating played an important role in the TPC start-up.

To understand the role of collisionless electrons in tokamak start-up, collisionless electron transport and their impact on magnetohydrodynamic (MHD) equilibrium need to be understood. The orbit-averaged Fokker-Planck simulation has been developed to study collisionless energetic electron transport during tokamak start-up when the field-lines are still open [8]. The Fokker-Planck simulation showed that the electrons were transported radially outward by EC waves due to finite orbit effects. On the TST-2 spherical tokamak, the losses due to this outward transport could explain the EC power and vertical field dependence of EC breakdown under the TPC. To study the impact of kinetic electron current on MHD equilibrium in rf start-up, equilibrium reconstruction code based on extended MHD has been developed [9,10]. The model was first applied to lower-hybrid start-up plasmas, and it was found that the kinetic electron current was necessary to accurately reproduce the magnetic and kinetic measurements.

In this work, we have studied the evolution of electron distribution function in EC assisted tokamak start-up starting from the vacuum TPC leading up to formation of the tokamak configuration with closed flux surfaces. Relativistic treatment was implemented to improve the accuracy of the description of EC heating. The global electron distribution function consistent with the experimental measurements was obtained for the first time by incorporating the results of the orbit-averaged Fokker-Planck simulation to the extended MHD equilibrium reconstruction.

NUMERICAL MODEL

The orbit-averaged distribution function was used to describe the collisionless kinetic electrons in this work. The orbits were labelled relativistically as follows:

$$\begin{split} \mathcal{E} &= mc^2(\gamma - 1) \simeq \frac{mv^2}{2} \\ \Lambda &= \frac{2\mu B_0}{mu^2} = \frac{B_0 u_\perp^2}{Bu^2} \simeq \frac{\mu B_0}{\mathcal{E}} \\ P_\phi &= q\left(\psi + \frac{RB_\phi}{\gamma\Omega}u_\parallel\right) = q\left(\psi + \frac{RB_\phi}{\Omega}v_\parallel\right) \end{split}$$

 \mathcal{E} is the kinetic energy, Λ relates to the velocity pitch angle, B_0 is an arbitrary magnetic field to normalize Λ and P_{ϕ} is the toroidal angular momentum. The approximate right most equality holds for non-relativistic energies. q and m are the particle charge and mass, respectively, v_{\parallel} and v_{\perp} are the velocity parallel and perpendicular to the equilibrium field, respectively, ψ is the poloidal flux, $\Omega = qB/(m\gamma)$ is the algebraic angular cyclotron frequency, $u = \gamma v$ is the normalized momentum where $\gamma = 1/\sqrt{1-v^2/c^2}$ and c is the speed of light.

The orbit-averaged Fokker-Planck simulation has been developed to study the transport of collisionless electrons [8]. The simulation can describe open field-lines to treat collisionless electron transport starting from the vacuum TPC. Finite orbit effects are included since the electron drift is not necessarily negligible at the start-up phase when the plasma current is low. For transport drive, quasilinear diffusion by rf waves, velocity space convection by toroidal DC electric field and Coulomb collisions by background plasma species were implemented. In this work, the model was upgraded to use relativistic description. For simulation of TST-2 start-up, EC quasilinear diffusion coefficients were calculated assuming uniform and isotropic electric fields based on the earlier experiments [11].

The extended MHD equilibrium reconstruction code has been developed to study the impact of kinetic electrons on MHD equilibrium [9,10]. The extended MHD model considers a two-component plasma of bulk MHD fluid and kinetic electrons described by an orbit-averaged distribution function. The extended MHD model was also upgraded to use relativistic description in this work. To include kinetic electron current by EC waves, we have implemented an analytic form of the orbit-averaged distribution function based on the Fokker-Planck simulation results. The overall coefficient of the kinetic electron current was treated as a fitting parameter to consistently reconstruct the equilibrium magnetic field and the global electron distribution function.

3. EXPERIMENTAL SETUP

TST-2 is a spherical tokamak ($R_0 = 0.36$ m, $\alpha = 0.23$ m, $B_{t0} < 0.3$ T) located at the University of Tokyo [12]. Five PF coil sets and the CS are driven by discharge of capacitor banks. The loop voltage for standard operation is < 5 V (< 2.2 V/m at the machine center). The discharge presented in this work had a low loop voltage of 0.7 V (0.31 V/m at the machine center). The EC heating system is powered by a 2.45 GHz magnetron with 5 kW source power. The EC waves were launched with X-mode polarization in this work, but the polarization is considered to be almost isotropic due to weak absorption [11]. The working gas was D₂. The machine is equipped with 50 pickup coils, 42 flux loops and Rogowski coils for plasma and coil currents for equilibrium reconstruction.

4. ANALYSIS OF ELECTRON DISTRIBUTION FUNCTION DURING TPC START-UP

4.1. Numerical simulation of electron transport under the TPC

Generation of collisionless energetic electrons by EC heating under the vacuum TPC was calculated with the orbit-averaged Fokker-Planck simulation. The momentum distribution function at the EC resonance layer R = 0.33 m on the midplane is shown in Fig. 1(a). The energetic electron tail formed in the direction perpendicular to the magnetic field. The high energy limit can be understood in terms of the electron orbits along the tail as shown in Fig. 1(b). The low-field side leg of the electron orbit expanded outwards as the electron energy increased, while the high-field side leg was pinned at the EC resonance. The upper limit of the confined electron energy was given by the condition where such an electron orbit touches the outer limiter, which occurred at around 1.3 keV for the vertical field strength of 0.5 mT.

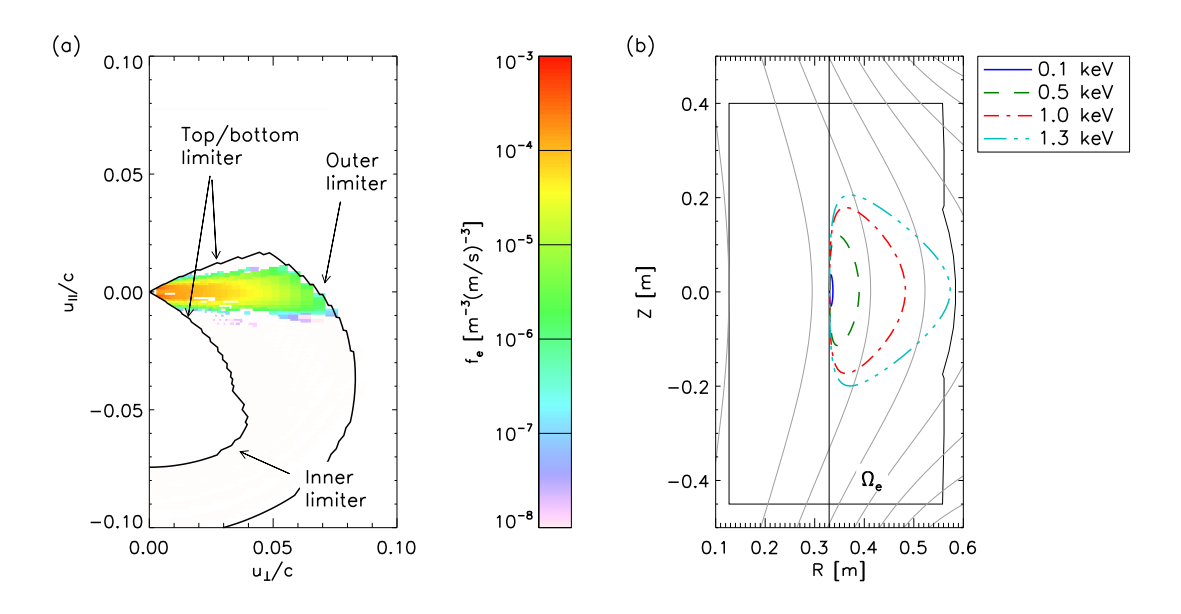


FIG. 1. (a) The momentum distribution function at R = 0.33 m (EC resonance layer) on the midplane from the orbit-averaged Fokker-Planck simulation. Vertical field strength 0.5 mT, EC electric field 0.4 kV/m and no loop voltage. Energetic electron tail formed in the perpendicular direction up to the boundary given by the orbit that touches the outer limiter. (b) Collisionless electron orbits with the turning points at the EC resonance on the midplane. The orbit expands to the low-field side with increasing energy until it touches the outer limiter at around 1.3 keV.

Figure 2 shows the result of the vertical field scan. The mean energy scaled approximately with the square of the vertical field strength due to the high momentum limit that was proportional to the vertical field strength. The plasma current scaled almost linearly with the vertical field strength, consistently with scaling expected from radial force balance. As a result, the ratio I_p/E , which can be considered a proxy of plasma current ramp rate per unit EC heating power, scaled inversely proportional to the vertical field strength. Relativistic effect reduced both mean energy E and plasma current I_p , and the ratio did not change significantly with relativistic correction.

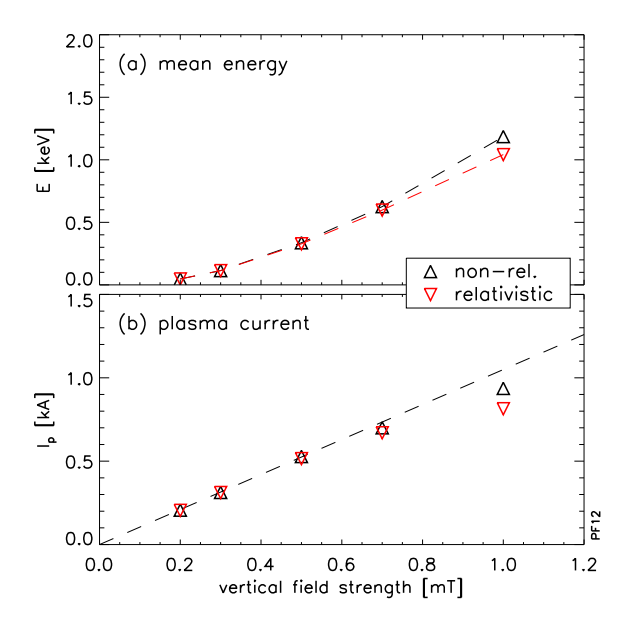


FIG. 2. The vertical field scan by the orbit-averaged Fokker-Planck simulation. No loop voltage. (a) The global mean energy. The dashed lines simply connect the simulated points represented by the symbols. (b) The total plasma current. The dashed line is the linear fit to the simulated points at low vertical field strength. Black upward triangles: non-relativistic electrons; red downward triangles: relativistic electrons.

The toroidal current density simulated with EC waves only and with both EC waves and loop voltage are shown in Fig. 3. Regardless of the presence of the loop voltage, a characteristic current profile to the low-field side of the EC resonance was predicted due to strong acceleration of electrons with the turning point at the EC resonance. When the loop voltage was applied, the electrons were transported to smaller pitch angle corresponding to greater P_{ϕ}/q . Strong perpendicular diffusion driven by EC waves resulted in strong phase-space transport to move the turning point of the trapped electrons to the EC resonance layer. The net result of combined DC electric field and EC waves was to transport trapped electrons towards greater ψ , which was towards the top and the bottom of the machine. In either case, EC quasilinear diffusion was the dominant driver, and the energetic electrons were generated to the low-field side of the EC resonance with a characteristic triangular kinetic current profile.

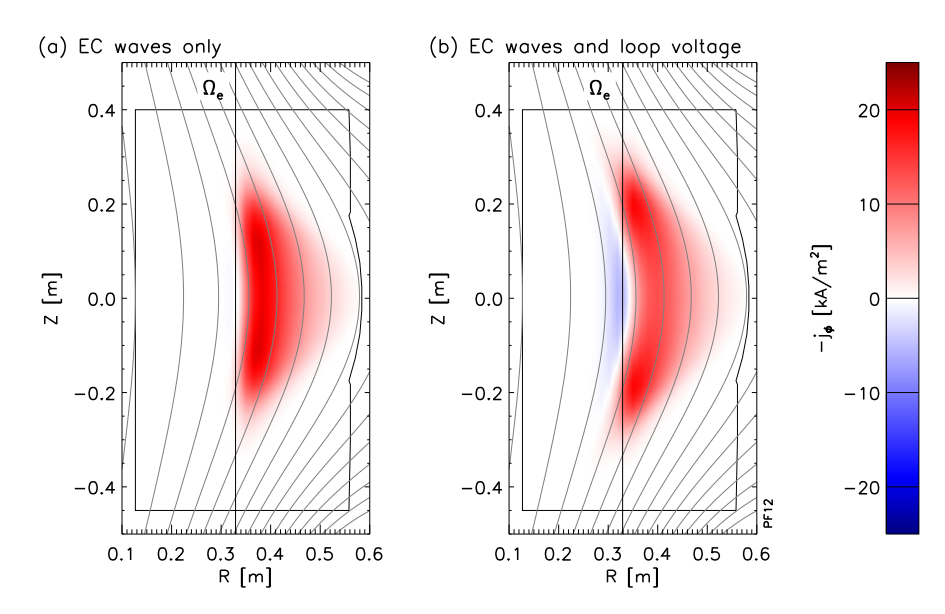


FIG. 3. Toroidal current density from the orbit-averaged Fokker-Planck simulation with EC waves only (a) and with EC waves and loop voltage of 0.5 V (b). Vertical field strength 1 mT. The EC resonance radius (0.32 m) is shown with the vertical lines. The grey solid curves are the poloidal flux contours.

4.2. Overview of the EC assisted Ohmic start-up discharge

EC assisted start-up experiments were performed on TST-2 to investigate the impact of the poloidal field configuration on start-up [6]. The overview of the time evolution of the EC assisted Ohmic start-up discharges is shown in Fig. 4. Start-up from the FNC and the TPC were compared for the same CS waveform, and therefore, the same volt-seconds. EC heating power and prefill deuterium pressure were also matched between the two discharges. EC power was applied from before initiation of breakdown throughout the plasma current ramp-up. Formation of closed flux surfaces was somewhere between 15 ms and 16 ms for the FNC when the vertical field at the outer radius turned positive (c) whereas the vertical field at the inner limiter was negative (g). For the TPC, in contrast, the vertical field at the inner limiter remained positive during the initiation of breakdown, and formation of closed flux surfaces could be identified clearly from the reversal of the inner limiter vertical field that occurred slightly before 15 ms. Burn-through was achieved for both configurations as can be seen in the D_{α} trace (f). However, the plasma current ramp-up was faster for the TPC case, resulting in substantially higher plasma current at the same CS volt-seconds.

Figure 5 shows the neutral pressure scan with the same CS waveform and EC heating power. At high pressure, little difference was observed between the FNC and the TPC. At low pressure, the TPC start-up was able to reach substantially higher plasma current, down to the lowest pressure where breakdown could not be obtained. The advantage of the TPC was that it could achieve prompt breakdown and fast plasma current rise immediately following the breakdown. This was the case particularly at high EC power and low neutral pressure which corresponded to low collisionality. In contrast, substantial breakdown delay and slow plasma current rise was observed for the FNC in low collisionality conditions. Large difference between the performance of the FNC and the TPC at low collisionality conditions suggested that collisionless electrons played an important role for the TPC start-up.

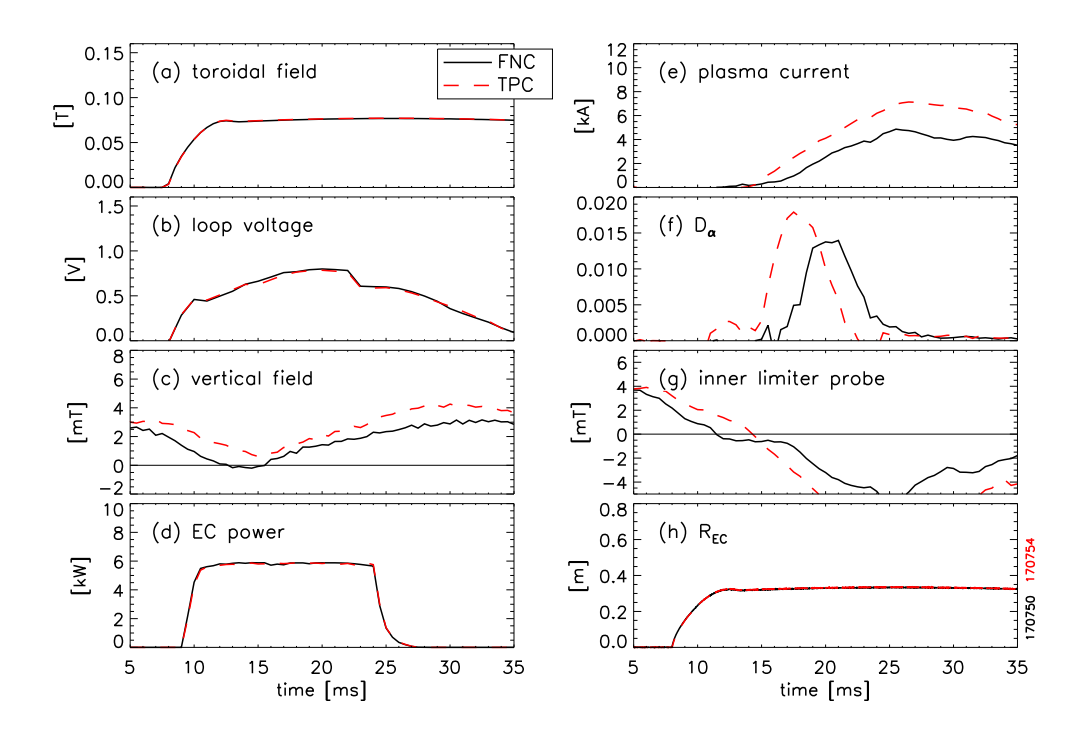


FIG. 4. The overview of the discharge time trace for start-up from the FNC (black solid) and the TPC (red dashed) in TST-2. Deuterium filling pressure was 6 mPa. (a) Toroidal field (b) loop voltage (c) vertical field strength at the machine center (d) EC heating power (e) plasma current (f) D_{α} radiation intensity (g) vertical field at the inner limiter on the midplane and (h) EC resonance radius. Plasma current ramp-up was faster for the TPC case. Reproduced with slight modification to the format from Fig. 6 of Ref. 6.

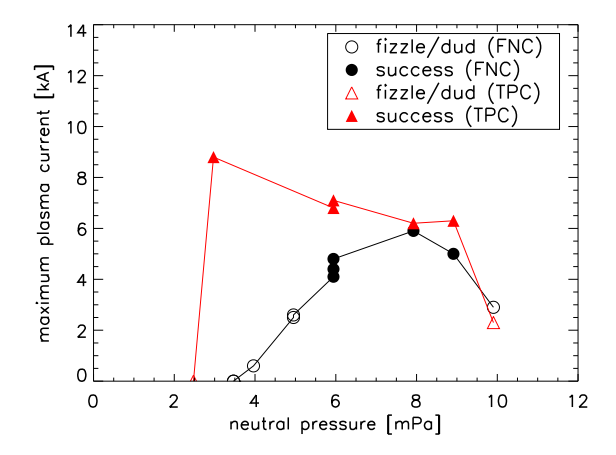


FIG. 5. The maximum plasma current achieved during the start-up phase for the FNC (black circles) and the TPC (red triangles) in TST-2. The CS waveform was fixed for all the discharges. EC power 5.0 kW and CS volt-seconds 0.013 Vs. The filled symbols are discharges with successful burn-through. Open symbols with zero plasma current at the lowest pressures did not breakdown (duds). Open symbols at higher pressure did not reach burn-through (fizzles). Reproduced with modification of the pressure unit from Fig. 7 of Ref. 6.

$\textbf{4.3. Numerical simulation of the global electron distribution function in EC assisted Ohmic start-up under the TPC\\$

The orbit-averaged distribution function was parameterized analytically as follows based on the Fokker-Planck simulation results presented in section 4.1:

$$f(\mathcal{E}, \Lambda, P_{\phi}) = \exp\left(-\frac{\mathcal{E}}{T} + \frac{\Lambda - \Lambda_{EC}}{\delta \Lambda}\right) \cos^2\left(\frac{\pi}{2} \frac{P_{\phi} - P_{EC}}{\delta P}\right) \text{ if } \Lambda < \Lambda_{EC} \text{ and } \left|P_{\phi} - P_{EC}\right| < \delta P \quad (1)$$

and zero otherwise. $\Lambda_{\rm EC}=eB_0/(m\omega)$ is the "resonant" value of the velocity pitch Λ that corresponds to the electrons with the turning point at the EC resonance. $P_{\rm EC}=q\psi_{\rm EC}$ where $\psi_{\rm EC}$ is the value of the poloidal flux at the intersection of the EC resonance layer and the midplane. The width in the Λ direction was set to be $\delta\Lambda=0.1\Lambda_{\rm EC},\ \delta P$ was set to q times the poloidal flux difference between the midplane and the top limiter and T=1 keV. The results of the extended MHD equilibrium reconstruction are shown in Fig. 6. Under the extended MHD model, the kinetic current carried by the trapped (and confined passing) electrons could naturally generate an equilibrium magnetic field that fitted the magnetic measurements including the time when the field-lines were still open. The evolution of the equilibrium magnetic field was obtained for the first time seamlessly from just after breakdown (a) until after closed flux surface formation (c).

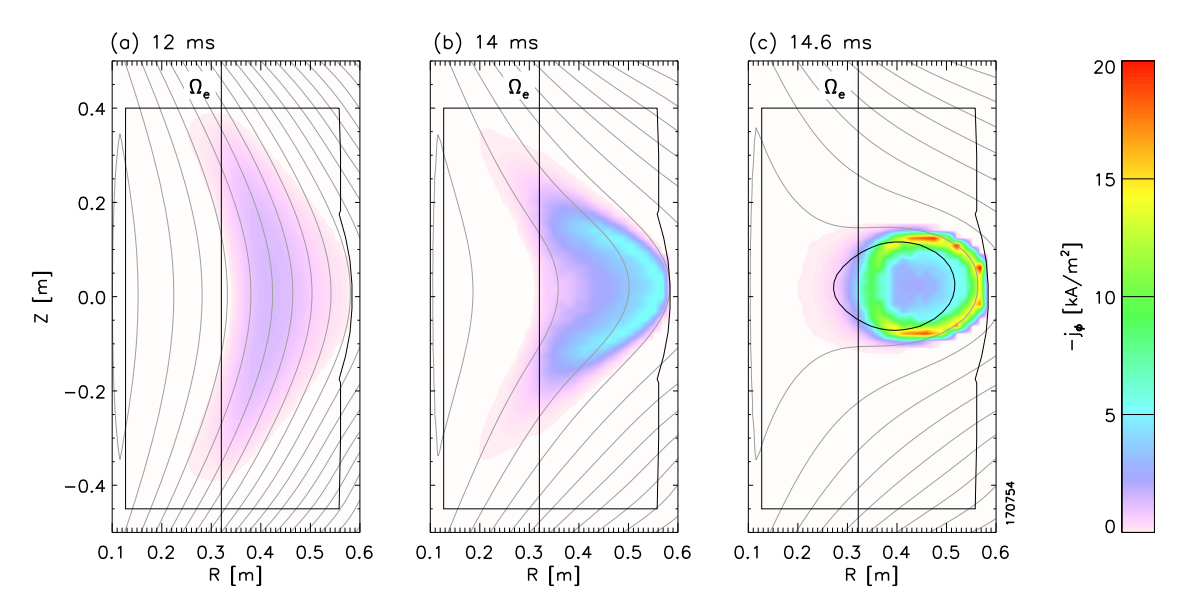


FIG. 6. The poloidal flux contours and the toroidal current profile from the extended MHD equilibrium reconstruction. The profiles are shown from just after the breakdown until after until after closed flux surfaces were formed. Reconstruction at (a) 12 ms (b) 14 ms and (c) 14.6 ms of the TPC discharge shown in Fig. 4. The vertical lines are the EC resonance layer. The solid black curve in (c) shows the last closed flux surface.

The poloidal profiles of moments calculated from the reconstructed distribution function are shown in Fig. 7. The pressure was anisotropic between the direction parallel and perpendicular to the magnetic field. The toroidal current was calculated using all three moments under the drift kinetic picture. In the present case, however, the diamagnetic current contribution was negligibly small. Since magnetic pitch was also small, $j_{\phi} \simeq -j_{\parallel}$. It can be seen that the kinetic current profile of the parametrized analytic distribution function (a) captures the characteristic current profile of the Fokker-Planck simulation shown in Fig. 3.

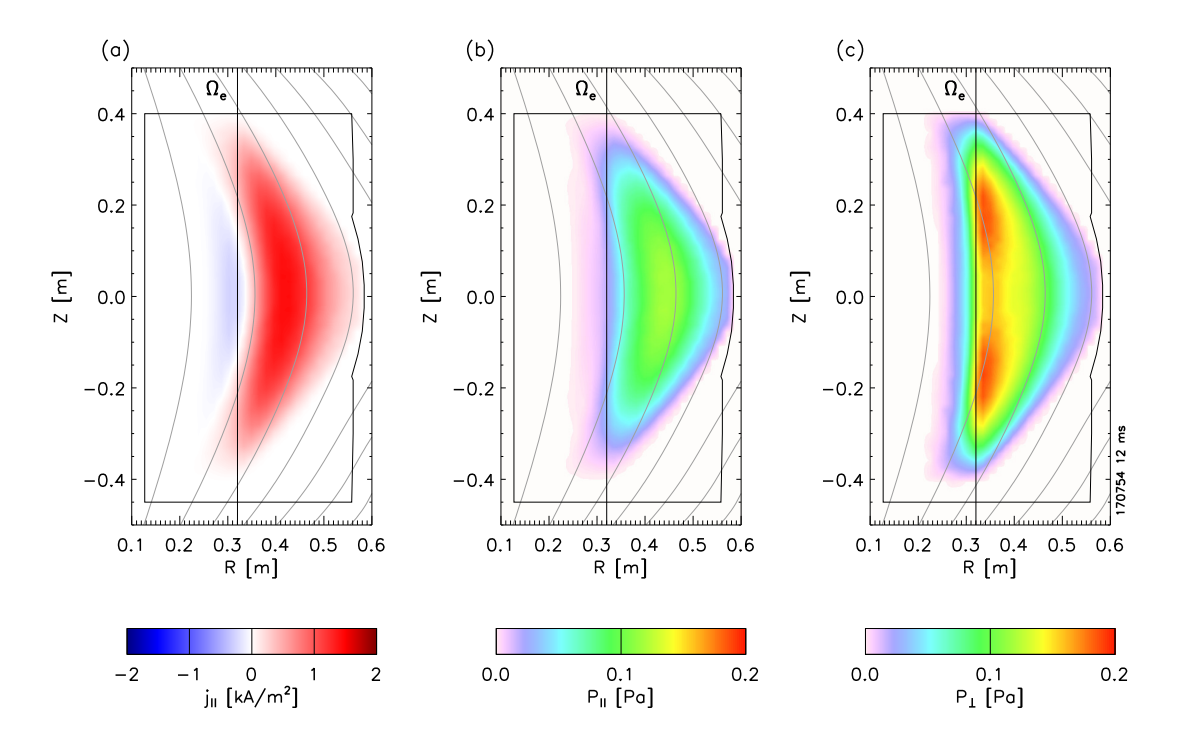


FIG. 7. The moments of the orbit-averaged distribution function obtained from the extended MHD equilibrium reconstruction. (a) The parallel current density (b) the parallel pressure and (c) the perpendicular pressure. The characteristic current profile from the Fokker-Planck simulation (Fig. 3) was captured with the analytic form of Eq. (1).

The Fokker-Planck simulation was performed again using the magnetic field obtained from the extended MHD equilibrium reconstruction (Fig. 6(a)). The distribution function simulated with and without the loop voltage is shown in Fig. 8. Energetic electrons were generated around the resonant pitch angle Λ_{EC} which is the condition for the electrons to have turning points at the EC resonance layer. In the presence of the loop voltage, convection by the DC electric field resulted in slight shift of the profiles to greater values of P_{ϕ}/q , similarly to what was observed earlier for the vacuum TPC in Fig. 3.

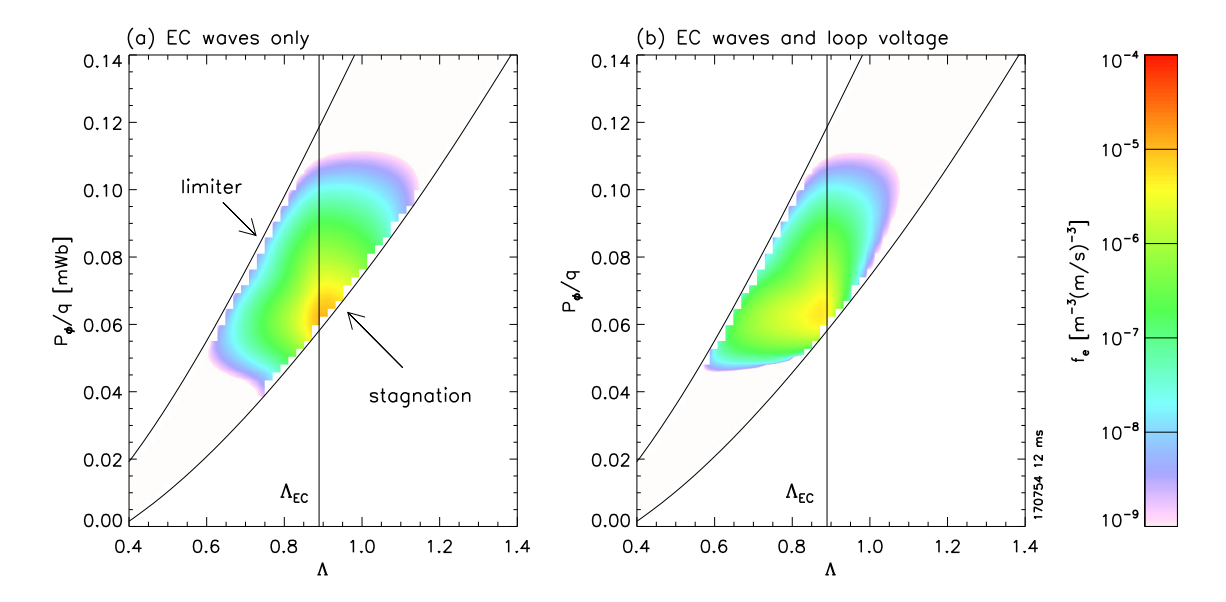


FIG. 8. The slice of the phase-space distribution function at 1 keV from the Fokker-Planck simulation with EC waves only (a) and with EC waves and loop voltage (b). Energetic electrons of 1 keV were observed around the resonant pitch Λ_{EC} shown with the vertical lines. The bulk temperature was set to 5 eV. When the loop voltage was applied, the distribution shifted slightly to greater P_{Φ}/q .

The Ohmic heating power was simulated to be localized around the EC resonance layer due to efficient acceleration of slightly energetic electron generated by EC waves. EC heating power was more than an order of magnitude greater than the Ohmic heating power. This is consistent with the fact that the simulated distribution function had a phase-space structure characteristic of EC heating regardless of the presence of the DC electric field typical for low loop voltage start-up conditions.

5. CONCLUSIONS

The extended MHD equilibrium reconstruction was applied to the EC assisted Ohmic start-up discharge on the TST-2 spherical tokamak to obtain equilibrium magnetic field and global electron distribution function consistent with the magnetic measurements. Time evolution of the equilibrium magnetic field and global electron distribution function was obtained consistently for the first time starting from the initial vacuum TPC leading to closed flux surface formation. The kinetic electron current under the TPC was shown to be sufficiently large to form closed flux surfaces under the typical EC heating power density on TST-2. Ohmic heating power density was localized around the EC resonance layer due to efficient DC electric field acceleration of energetic electrons generated by EC waves. The Ohmic heating power was more than an order of magnitude smaller than the EC heating power throughout the early start-up phase up to closed flux surface formation. The distribution function was simulated to have a characteristic form resulting from tail formation of electrons with turning points at the EC resonance layer regardless of the presence of the DC electric field under the low loop voltage start-up conditions.

ACKNOWLEDGEMENTS

We thank Dr. T. Wakatsuki, Dr. M. Yoshida, Dr. H. Urano for valuable discussions over the course of this work. Special thanks to Dr. Y. Ko for conducting the experiments that formed the basis of this work.

REFERENCES

- [1] LLOYD, B., et al., Low voltage Ohmic and electron cyclotron heating assisted startup in DIII-D, Nucl. Fusion **31** (1991) 2031.
- [2] FOREST, C.B., et al., Internally generated currents in a small-aspect-ratio tokamak geometry, Phys. Rev. Lett. **68** (1992) 3559.
- [3] FOREST, C.B., et al., Investigation of the formation of a fully pressure driven tokamak, Phys. Plasmas 1 (1994) 1568.
- [4] AN, Y., et al., Efficient ECH-assisted plasma start-up using trapped particle configuration in the versatile experiment spherical torus, Nucl. Fusion 57 (2016) 016001.
- [5] LEE, J., et al., Study on ECH-assisted start-up using trapped particle configuration in KSTAR and application to ITER, Nucl. Fusion **57** (2017) 126033.
- [6] KO, Y., et al., Optimization of Poloidal Field Configuration for Electron Cyclotron Wave Assisted Low Voltage Ohmic Start-Up in TST-2, Plasma Fusion Res. **16** (2021) 1402056.
- [7] WAKATSUKI, T., et al., Achievement of the first tokamak plasma with low inductive electric field in JT-60SA, Nucl. Fusion **64** (2024) 104003.
- [8] TSUJII, N., et al., Kinetic Analysis of the Characteristics of Electron Cyclotron Heating Assisted Ohmic Start-Up in the Trapped Particle Configuration of a Tokamak, Plasma Fusion Res. **18** (2023) 1402051.
- [9] TSUJII, N., et al., Modification of the magneto-hydrodynamic equilibrium by the lower-hybrid wave driven fast electrons on the TST-2 spherical tokamak, Nucl. Fusion **61** (2021) 116047.
- [10] TSUJII, N., et al., Studies of the outer-off-midplane lower hybrid wave launch scenario for plasma start-up on the TST-2 spherical tokamak, Nucl. Fusion **64** (2024) 086017.
- [11] SUGIYAMA, J., et al., Electron Cyclotron Heating Start-Up Experiments on TST-2, Plasma Fusion Res. 3 (2008) 026.
- [12] TAKASE, Y., et al., Initial results from the TST-2 spherical tokamak, Nucl. Fusion 41 (2001) 1543.